



Artificial Intelligence Using FFNN Models for Computing Soil Complex Permittivity and Diesel Pollution Content

Hamsa Nimer ¹, Rabah Ismail ², Adnan Rawashdeh ³, Hashem Al-Mattarneh ^{1*},
Mohanad Khodier ¹, Randa Hatamleh ¹, Musab Abuaddous ¹

¹ Department of Civil Engineering, Yarmouk University, Irbid 21163, Jordan.

² Department of Civil Engineering, Jadara University, Irbid 21110, Jordan.

³ Faculty of Computer Sciences and Information Technology, Yarmouk University, Irbid, 21163, Jordan.

Received 11 May 2024; Revised 08 August 2024; Accepted 13 August 2024; Published 01 September 2024

Abstract

Soil pollution caused by hydrocarbons, such as diesel, poses significant risks to both human health and the ecosystem. The evaluation of soil pollution and various soil engineering applications often relies on the analysis of complex permittivity, encompassing parameters such as dielectric constant and dielectric loss. Various computational models, including theoretical physics-based models, mixture theory models, statistical empirical models, and artificial neural network (ANN) models, have been explored for computing soil complex permittivity and predicting water and pollutant content. Theoretical models require detailed data that is often unavailable, and thus have limited applicability. Mixture models tend to underestimate soil characteristics due to inaccuracies in permittivity estimation of soil phases. While empirical models are widely used, their applicability is restricted to specific soil types, datasets, and locations. ANN models offer promising predictions, accommodating nonlinear phenomena and allowing for missing information and variables. In this study, capacitive electromagnetic electrode sensors were utilized to determine the complex permittivity of soil contaminated with varying levels of diesel at different moisture levels. Theoretical mixture, empirical, and Feed Forward Neural Network (FFNN) models were employed to compute the permittivity of polluted soil based on its phases and to predict the level of diesel pollution. A comparison of these modeling approaches revealed that the FFNN model exhibited the best performance. The ANN model demonstrated superior performance metrics, including a high correlation coefficient and lower mean square error. Specifically, the correlation coefficients for the FFNN model were 0.9942 for training samples, 0.9967 for validation samples, and 0.9977 for test samples. Additionally, the ANN model yielded the lowest mean square error compared to the other three models.

Keywords: Complex Permittivity; Dielectric Properties; Soil; Diesel Contamination; Water Content; Artificial Neural Network; Artificial Intelligence.

1. Introduction

Soil pollution poses a worldwide concern and serious threat. Since soil plays a pivotal role in furnishing a multitude of ecosystem services vital for the preservation of life on our planet, its contamination presents significant risks to both human and ecosystem well-being [1, 2]. Petroleum products like diesel, kerosene, and crude oil from the oil industry, along with leakage from oil reservoirs, can all contaminate soil. The widespread recognition of soil contaminated with these wastes as a severe issue has prompted global concern. The type and concentration of soil pollution brought on by human activity have steadily increased in recent years with the expansion of the global economy. This has led to the

* Corresponding author: hashem.mattarneh@yu.edu.jo

<http://dx.doi.org/10.28991/CEJ-2024-010-09-018>



© 2024 by the authors. Licensee C.E.J, Tehran, Iran. This article is an open access article distributed under the terms and conditions of the Creative Commons Attribution (CC-BY) license (<http://creativecommons.org/licenses/by/4.0/>).

degradation of some ecosystems. Worldwide, there are many incidents of spills of diesel fuel and other hydrocarbon-type oils from storage facilities, underground tanks, pipeline ruptures, and leakage from heavy equipment [3]. These spills onto the ground surface are sources of widespread soil and water pollution. The extent of contamination depends on the characteristics of the hydrocarbon spilled, the water content of the soil, and the soil type and characteristics. Cleaning up after an event can prove very expensive. Therefore, it is critical to develop quick computing, modeling, and non-destructive techniques for determining the level of hydrocarbon contamination and forecasting the effectiveness of clean-up efforts [4].

Over the past 20 years, the concept of complex permittivity of materials has been widely applied. A variety of geophysical electromagnetic techniques can be employed to ascertain the dielectric characteristics of materials, including soil [5]. These techniques include noncontact free-space microwave techniques [6, 7], near-field waveguide microwave methods [8-10], time domain reflectometers [11], ground penetration radar [12], capacitive electrode methods, and parallel disk electrodes [13-15]. To extract the complex permittivity of soil, all of these methods use electromagnetic signals to excite the soil material and then measure the parameters of the signal change by the soil material. The physical characteristics and composition of soil material can be linked to its complex permittivity characteristics, which are known as the dielectric constant and dielectric loss. This relationship can be used to estimate soil properties, like moisture content, density, and types of contamination, in a non-destructive way [16, 17]. Electromagnetic methods have been used for the advanced characterization of several materials, including cement concrete, asphalt concrete, composites, and both clean and wastewater. Electromagnetic methods are used extensively in soil and geotechnical applications based on their measured dielectric constant and dielectric loss [18-20]. The electromagnetic sensing of soil material, particularly for pollution and moisture content, still requires the development of electromagnetic sensors that can be used both in the lab and in the field under similar conditions. This approach can help avoid discrepancies between lab and field sensor designs and setups. Moreover, developing such sensors can eliminate the differences in soil conditions between lab and field, known as disturbed and undisturbed samples [21, 22].

The relationship between dielectric properties and soil composition is determined using theoretical dielectric models, including mixture theory and phonological models, and empirical models using central composite and response surface methodologies. There are several problems associated with these models and methods, such as complications of soil material, unavailability of needed soil information, complicated nonlinear relationships, and the limited application of the statistical methods to the condition of soil used to develop these models.

ANN shows promising capabilities of overcoming such problems in many fields [23]. ANN models have been used for several applications for the prediction of the composition of various materials, including soil. ANN has been found to offer good modeling techniques in many areas of soil material, including the prediction of soil consolidation [24], prediction of soil organic matter [25], estimation of the shear strength of soil [26], prediction of soil compaction [27, 28], prediction of soil permeability [29], estimation of soil moisture [30], and soil pollution from materials such as heavy metals and hydrocarbons [31, 32]. ANN has the potential to model the dielectric properties of soil material and predict moisture and diesel pollution content. However, limited research has been conducted using ANN for soil material, and no studies are currently available that focus on soil diesel contamination and soil moisture content [31, 32].

This study was conducted with the aim of addressing the gaps in soil sensing and enhancing the dielectric modeling of soil material, particularly for quantifying pollution content and moisture. The approach includes theoretical, empirical, and ANN methods. This paper presents the experimental preparation of soil material contaminated with diesel at various moisture contents. A capacitive electromagnetic electrode sensor was used to compute soil complex permittivity at various diesel contamination levels and at different soil water contents. This study also computes the complex permittivity of the contaminated soil using theoretical dielectric models. Moreover, it determines the relationship between the soil phases, such as water content and diesel contamination level, and the measured dielectric properties of the soil. Finally, the study investigates the use of different ANN models to compute the soil dielectric properties at various contamination levels and predict its water and diesel content. A comparison of all these theoretical, empirical, and ANN models for soil pollution application was also conducted.

2. Dielectric Modeling and Computing of Soil Material

The complex permittivity (ϵ^*) of materials such as soil is a measure of the ability of a material to store energy from an electric field. It is related to the more familiar concepts of dielectric constant (DC or ϵ') and dielectric loss (DL or ϵ''). The relative permittivity is the ratio of the electric displacement in a soil material to the electric field. It is a fundamental parameter in electromagnetics as it measures how much the soil material opposes the formation of an electric field inside it, as well as how well the material transmits an electric field through itself. The relationship between the relative permittivity (ϵ^*) and the real (DC or ϵ') and imaginary parts (DL or ϵ'') of the dielectric or permittivity is given by the following Equation in which j is an imaginary number ($\sqrt{-1}$) [33].

$$\epsilon_{soil}^* = \epsilon'_{soil} - j\epsilon''_{soil} \quad (1)$$

Three approaches, namely the phenomenological approach, mixture volumetric approach, and empirical statistical approach, have been used to develop several theoretical and empirical physical dielectric models [34-36]. These three approaches are briefly explained as follows:

2.1. Phenomenological Approach

Reviewing phenomenological models like Cole-Cole [37] and Debye [38] makes it clear that each unique material needs to be recalibrated. It is evident that these models fail to explain the dielectric differences between various soil types and, consequently, they are not applied in practice for soil moisture prediction [36, 39].

2.2. Mixture Volumetric Approach

Volumetric mixture models characterize the soil's dielectric properties based on the relative concentrations of its constituents, each of which has unique dielectric properties. The four main input parameters that these models use are pore space, volumetric water content, diesel contamination content, and solid matter [40]. Several volumetric models of four-phase mixtures were developed for soil moisture content. These phases comprise air, water, diesel, and solid particles. The volume fractions of these phases are volume of air (θ_a), volume of water (θ_w), volume of diesel (θ_d), and volume of soil solid particles (θ_s). The corresponding dielectric properties for these four soil phases are needed to compute soil dielectric properties. The most popular theoretical mixture models for calculating the moisture content and contamination content of soil are as follows:

It was suggested to use Silberstein's linear model [41]. The dielectric constant (DC or ϵ') and loss factor (DL or ϵ'') formulas are given by Equations 2 and 3, respectively.

$$DC = \epsilon'_{soil} = \theta_s \epsilon'_s + \theta_w \epsilon'_w + \theta_d \epsilon'_d + \theta_a \epsilon'_a \quad (2)$$

$$DL = \epsilon''_{soil} = \theta_s \epsilon''_s + \theta_w \epsilon''_w + \theta_d \epsilon''_d + \theta_a \epsilon''_a \quad (3)$$

According to Birchak's square root model (power = 0.5) [42], the dielectric constant and dielectric loss formulas are given by Equations 4 and 5, respectively.

$$\sqrt{DC} = \sqrt{\epsilon'_{soil}} = \theta_s \sqrt{\epsilon'_s} + \theta_w \sqrt{\epsilon'_w} + \theta_d \sqrt{\epsilon'_d} + \theta_a \sqrt{\epsilon'_a} \quad (4)$$

$$\sqrt{DL} = \sqrt{\epsilon''_{soil}} = \theta_s \sqrt{\epsilon''_s} + \theta_w \sqrt{\epsilon''_w} + \theta_d \sqrt{\epsilon''_d} + \theta_a \sqrt{\epsilon''_a} \quad (5)$$

According to Looyenga's power model (power = 1/3) [43], the dielectric constant and dielectric loss formulas are given by Equations 6 and 7, respectively.

$$DC = (\epsilon'_{soil})^{1/3} = \theta_s (\epsilon'_s)^{1/3} + \theta_w (\epsilon'_w)^{1/3} + \theta_d (\epsilon'_d)^{1/3} + \theta_a (\epsilon'_a)^{1/3} \quad (6)$$

$$DL = (\epsilon''_{soil})^{1/3} = \theta_s (\epsilon''_s)^{1/3} + \theta_w (\epsilon''_w)^{1/3} + \theta_d (\epsilon''_d)^{1/3} + \theta_a (\epsilon''_a)^{1/3} \quad (7)$$

Lichtenecher has proposed a logarithmic model [44] in which the dielectric constant and dielectric loss formulas are given by Equations 8 and 9, respectively.

$$DC = \epsilon'_{soil} = \theta_s \ln \epsilon'_s + \theta_w \ln \epsilon'_w + \theta_d \ln \epsilon'_d + \theta_a \ln \epsilon'_a \quad (8)$$

$$DL = \epsilon''_{soil} = \theta_s \ln \epsilon''_s + \theta_w \ln \epsilon''_w + \theta_d \ln \epsilon''_d + \theta_a \ln \epsilon''_a \quad (9)$$

Among these mixture models, a general power model was used for several materials with different powers. The researcher sought to determine the power value that best fits the experimental data. The power mode for the dielectric constant and dielectric loss are given by Equations 9 and 10, respectively.

$$(DC)^\alpha = (\epsilon'_{soil})^\alpha = \theta_s (\epsilon'_s)^\alpha + \theta_w (\epsilon'_w)^\alpha + \theta_d (\epsilon'_d)^\alpha + \theta_a (\epsilon'_a)^\alpha \quad (10)$$

$$(DL)^\alpha = (\epsilon''_{soil})^\alpha = \theta_s (\epsilon''_s)^\alpha + \theta_w (\epsilon''_w)^\alpha + \theta_d (\epsilon''_d)^\alpha + \theta_a (\epsilon''_a)^\alpha \quad (11)$$

For all these mixture models, the volume fraction of the soil phases and the dielectric properties of each phase are required. Moreover, these models are unreliable for estimating the soil moisture content because they do not account for the interactions between the soil phases. There could be a chemical or physical interaction between the water phase and the soil solid particles phase. However, none of the previous models has considered the existence of such interactions.

2.3. The Statistical and Empirical Approach

An empirical model is a statistical and mathematical representation of the relationships between the dielectric properties of a medium and its other characteristics, such as its texture and volumetric water content. In such models, the physical basis for the mathematical description is usually ignored. Therefore, an empirical model might only be valid for the data that is used to establish the relationship. Several empirical models have been developed from the study of soil moisture content. Numerous models put forth by researchers are dependent on their data fitting, model parameter

calculation, and experimental work. Empirical models lack a standard formula; instead, it is necessary to conduct numerous trials in order to determine which statistical regression model best fits the data. One must conduct an ANOVA analysis and determine the correlation coefficient, error, F-test, and level of significance in order to choose the best model from among the trials. Topp [45] presented the most widely used empirical dielectric model for soil moisture content. Topp's model cannot accurately measure the dielectric properties of soil when it contains organic matter, has a varied texture, or possesses other characteristics. Topp's formula is given in Equation 12 and could be rewritten in the form of Equation 13 [46].

$$\theta_w = -0.053 + 0.0292(\varepsilon'_{soil}) - 5.5 \times 10^{-4}(\varepsilon'_{soil})^2 + 4.3 \times 10^{-6}(\varepsilon'_{soil})^3 \quad (12)$$

$$DC = \varepsilon'_{soil} = 3.03 + 9.30(\theta_w) + 146.0(\theta_w)^2 - 76.70(\theta_w)^3 \quad (13)$$

Using response surface methodology with factorial analysis or central composite design of experiments, quadratic empirical models can be a useful tool to fit many engineering problems [47, 48]. The quadratic model can be presented by Equation 14.

$$Y = \beta_0 + \sum_{i=1}^k \beta_i x_i + \sum_{i=1}^k \sum_{j=i+1}^k \beta_{ij} x_i x_j + \sum_i \beta_{ii} x_i^2 + e \quad (14)$$

If this Equation is applied to soil with two factors ($k=2$), such as water content ($X_i=\theta_w$) and diesel content ($X_j=\theta_d$), this quadratic formula can be used to generate 4 models, namely the linear, pure quadratic, interaction, and full quadratic models. These four models are given by Equations 15 to 18, respectively.

$$\varepsilon'_{soil} = \beta_0 + \beta_1 \theta_w + \beta_2 \theta_d \quad (15)$$

$$\varepsilon'_{soil} = \beta_0 + \beta_1 \theta_w + \beta_2 \theta_d + \beta_{11} \theta_w^2 + \beta_{22} \theta_d^2 \quad (16)$$

$$\varepsilon'_{soil} = \beta_0 + \beta_1 \theta_w + \beta_2 \theta_d + \beta_{12} \theta_w \theta_d \quad (17)$$

$$\varepsilon'_{soil} = \beta_0 + \beta_1 \theta_w + \beta_2 \theta_d + \beta_{11} \theta_w^2 + \beta_{22} \theta_d^2 + \beta_{12} \theta_w \theta_d \quad (18)$$

The four models can be written for dielectric loss by Equations 19 to 22.

$$\varepsilon''_{soil} = \beta_0 + \beta_1 \theta_w + \beta_2 \theta_d \quad (19)$$

$$\varepsilon''_{soil} = \beta_0 + \beta_1 \theta_w + \beta_2 \theta_d + \beta_{11} \theta_w^2 + \beta_{22} \theta_d^2 \quad (20)$$

$$\varepsilon''_{soil} = \beta_0 + \beta_1 \theta_w + \beta_2 \theta_d + \beta_{12} \theta_w \theta_d \quad (21)$$

$$\varepsilon''_{soil} = \beta_0 + \beta_1 \theta_w + \beta_2 \theta_d + \beta_{11} \theta_w^2 + \beta_{22} \theta_d^2 + \beta_{12} \theta_w \theta_d \quad (22)$$

3. Artificial Intelligence Using ANN for Soil Application

Modeling and computing are the process of transforming one type of information into another desired format using instructions and procedures. The advent of technology has positioned computer-aided design methods as promising tools for simulating a wide range of engineering challenges. In this technological age, researchers worldwide are actively exploring the integration of machine learning, deep learning, and artificial intelligence into these processes. Numerous methods have been developed during the last three decades under the umbrella of artificial intelligence. Some methods mimic physiological functions, such as neural connections. In contrast, the others utilize strategies that rely less on natural processes and more on mathematical, logical, and statistical processes. All facets of computational intelligence are included in the broad field of artificial intelligence.

ANNs are information-processing systems whose architectures closely resemble the biological structure of the brain [49]. In situations where it is difficult to establish numerical equations due to diversity, ANNs have been successfully used to link independent variables to a series of dependent ones. In the past few years, ANNs have been employed more frequently in a variety of geotechnical engineering fields, including soil liquefaction [50], foundation settlements [49], and soil compaction characteristics [51]. ANNs are among the information-driven modeling tools that may capture complicated and nonlinear interactions between input and output datasets without requiring a prior understanding of the underlying phenomena. ANNs have a flexible statistical structure. Three or more layers are usually present in these networks: an input layer, hidden layers, and an output layer. The neurons of the primary hidden layer receive all its input data from the input layer [52]. When producing outputs that match predetermined inputs, the output layer is essential. In the meantime, sets of feature detectors are performed by the hidden layers, which might consist of one or more layers. In system modeling, choosing the right network framework is an important but difficult challenge. A schematic illustration of a general 3-layer ANN model is shown in Figure 1.

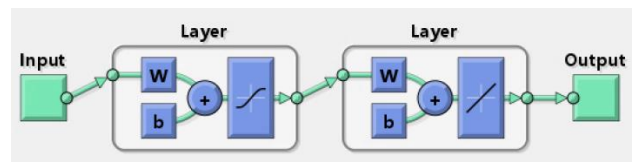


Figure 1. A schematic representation of a general 3-layer ANN model

Applying ANNs can be done in a variety of ways, and deducing which one works best is challenging because it involves systematically testing a lot of different scenarios. There are several different types and frameworks of ANNs, such as Regression Neural Networks, Multilayer Perceptron Networks, Probabilistic Neural Networks, Radial Functions Networks (RFN), Back Propagation Networks (BPN), and Feedforward Neural Networks (FFNNs). The most widely used of these are FFNNs, BPNs, and RFNs [53].

The creation of an ANN model to investigate the connections between soil complex permittivity and the four soil phases (solid, water, air, and diesel contamination) is one of the study's two primary goals. To control soil pollution and assess the total pollution level, it is essential to comprehend the relationship between soil dielectric constant, dielectric loss, and volume fraction of soil phases. The second goal is to employ the ANN to forecast the degree of soil contamination by using the soil's measured dielectric constant and dielectric loss.

4. Experimental Program

The methodology used in this study is summarized in Figure 2.

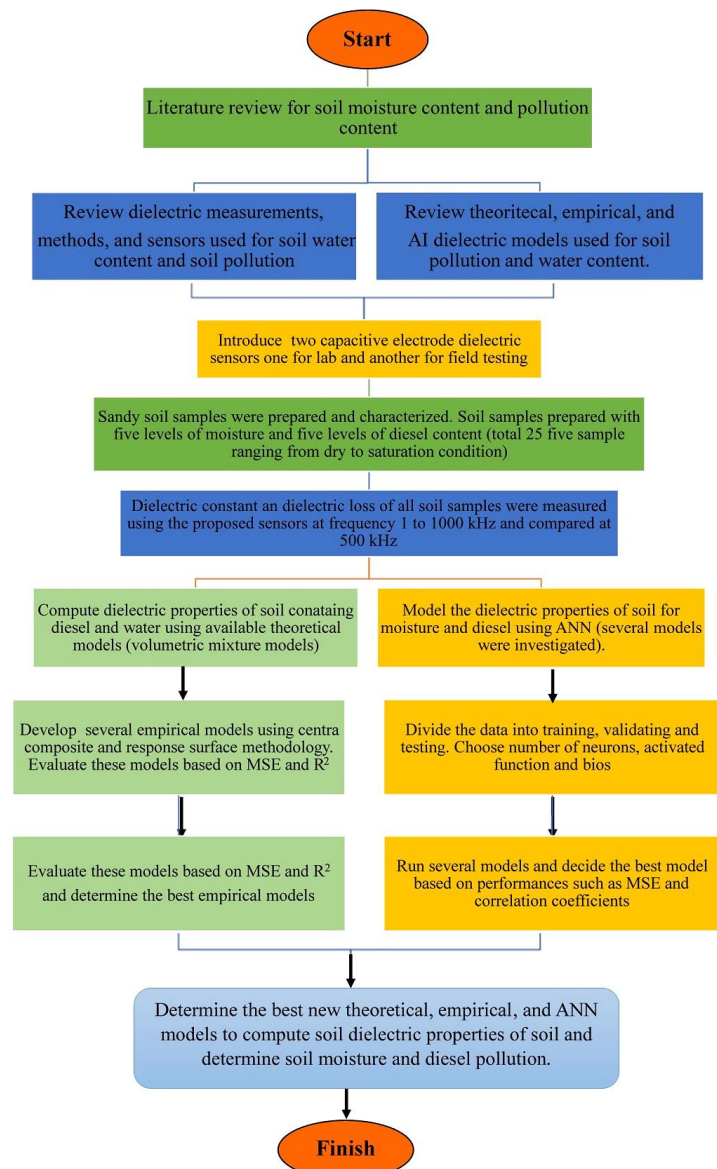


Figure 2. Flowchart showing the research methodology conducted in this study

4.1. Material Properties

A sample of sandy soil was used in this study. The grain size distribution of the soil and the factorial analysis of the soil moisture and diesel are given in Figure 3. Table 1 shows the properties of 500 g of sandy soil used in this study. The diesel used in this study was supplied by Jo-Petrol Co. with a density equal to 0.845 g/m³. The properties of the used diesel and sand are given in Table 1.

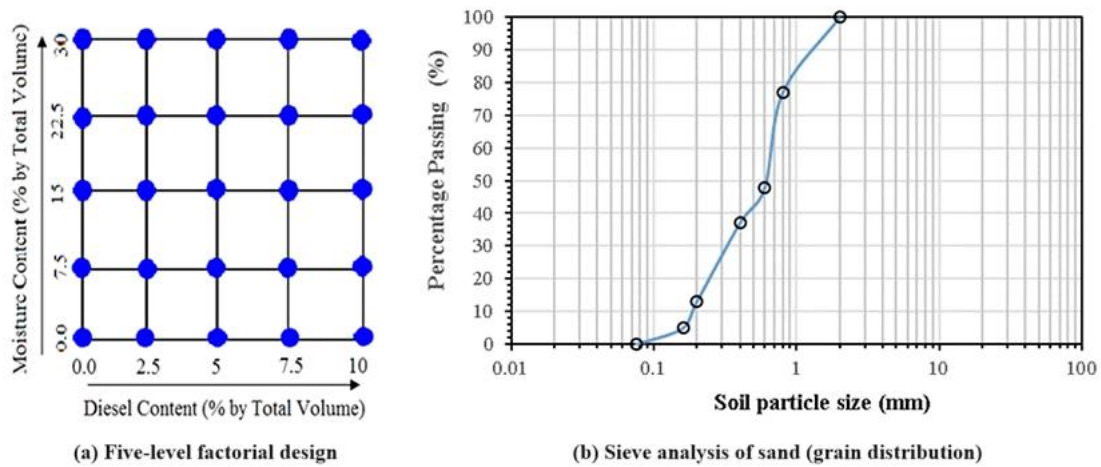


Figure 3. Properties of the soil samples (a) Five-level factorial design for moisture and diesel content; (a) factorial design and (b) grain distribution of the soil samples

Table 1. The properties of the soil and diesel used in this study

Properties	Sandy Soil	Properties	Diesel Pollutant
Total volume (V) of the dry sample (cm ³)	315.66	Polycyclic aromatic hydrocarbons (Mass %)	8%
Volume of solid (cm ³)	189.39	Flash Point (°C)	> 55°C
Volume of voids (Vv) (cm ³)	126.26	Sulfur Content (Mass %)	0.7%
Porosity	0.4	Cetane Index	46
Specific gravity (Gs)	2.64	Cetane Number	51
Bulk density (g/cm ³)	1.584	Density at 15°C (kg/m ³)	845

4.2. Capacitive Electrode Dielectric Sensor

The complex permittivity of the polluted soil, including the real term called dielectric constant (DC or ϵ') and the imaginary term known as dielectric loss (DL or ϵ''), were measured using the capacitive parallel electrode sensor for lab (CPES-L) developed in previous studies [21]. Figure 4 shows the schematic diagram of CPES-L and the actual sensor. Figure 5 shows the soil container and the cell filled with polluted soil during testing. This CPES-L can be used to measure the dielectric properties of soil in the lab. Another set of capacitive electromagnetic electrode sensors (CPES-F) were developed to measure the permittivity of soil in the field. Samples of these sensors are shown in Figure 6 [23]. The volume fraction and dielectric properties of the soil samples at various moisture content and different diesel content are given in Table 2. All the results of DC and DL were measured at a frequency range from 1 kHz to 1000 kHz. The results in Table 2 were measured at a frequency level of 500 kHz.

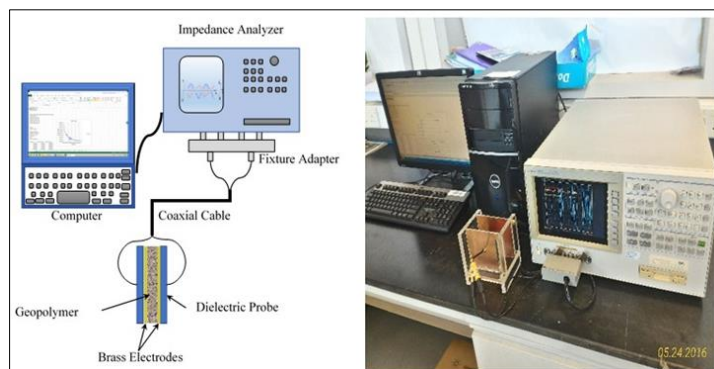
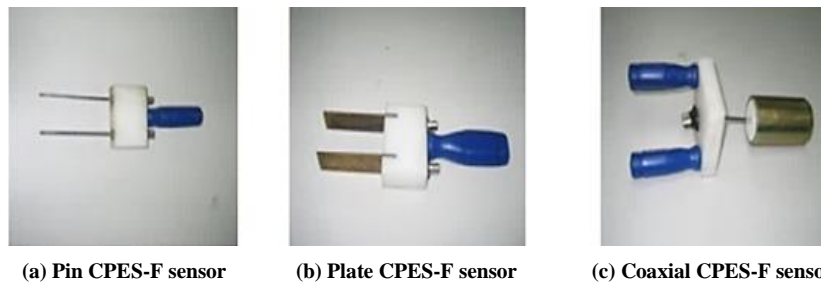


Figure 4. CPES-L operating in a low frequency from 1 kHz to 30 MHz (a) A schematic diagram of the (a) schematic diagram of the CPES-L; (b) The actual CPES-L



Figure 5. Soil sample during lab testing to measure soil dielectric properties



(a) Pin CPES-F sensor (b) Plate CPES-F sensor (c) Coaxial CPES-F sensor

Figure 6. Capacitive parallel electrode sensors for field (CPES-F)

Table 2. The properties of the soil and diesel used in this study

Code of soil samples	Solid θ_s	Water θ_w	Air θ_a	Diesel θ_d	DC (ϵ')	DL (ϵ'')
D0W0	0.600	0.000	0.400	0.000	2.327	0.362
D1W0	0.600	0.000	0.375	0.025	2.811	0.034
D2W0	0.600	0.000	0.350	0.050	2.951	0.025
D3W0	0.600	0.000	0.325	0.075	3.041	0.016
D4W0	0.600	0.000	0.300	0.100	3.075	0.065
D0W1	0.600	0.075	0.325	0.000	6.875	20.204
D1W1	0.600	0.075	0.300	0.025	7.183	23.946
D2W1	0.600	0.075	0.275	0.050	8.900	31.649
D3W1	0.600	0.075	0.250	0.075	8.748	31.972
D4W1	0.600	0.075	0.225	0.100	8.680	30.329
D0W2	0.600	0.150	0.250	0.000	10.344	38.164
D1W2	0.600	0.150	0.225	0.025	10.956	42.071
D2W2	0.600	0.150	0.200	0.050	12.590	45.210
D3W2	0.600	0.150	0.175	0.075	15.040	55.720
D4W2	0.600	0.150	0.150	0.100	15.600	60.400
D0W3	0.600	0.225	0.175	0.000	14.900	64.000
D1W3	0.600	0.225	0.150	0.025	17.000	70.000
D2W3	0.600	0.225	0.125	0.050	22.000	79.200
D3W3	0.600	0.225	0.100	0.075	24.400	81.800
D4W3	0.600	0.225	0.075	0.100	26.000	92.200
D0W4	0.600	0.300	0.100	0.000	23.700	122.000
D1W4	0.600	0.300	0.075	0.025	23.100	140.000
D2W4	0.600	0.300	0.050	0.050	27.000	131.000
D3W4	0.600	0.300	0.025	0.075	30.000	119.000
D4W4	0.600	0.300	0.000	0.100	29.100	118.289

4.3. Performance Criteria Used To Evaluate The Computing Models

To validate the performance of the computed models developed in this study, several quantitative parameters were used, including mean square error (MSE) and correlation coefficient of fitting (R). These parameters were calculated using the formulas given in Equations 23 and 24.

$$MSE = \sqrt{\frac{1}{n} \sum_{i=1}^n (O_i - \bar{O}_i)^2} \tag{23}$$

$$R = \sqrt{1 - \frac{\sum_{i=1}^n (O_i - \bar{O}_i)^2}{\sum_{i=1}^n (O_i - \bar{O})^2}} \tag{24}$$

where O_i is the actual and measured output, \bar{O}_i is the computed and predicted output using the proposed model, \bar{O} is the mean value of the output O_i , and n is the number of soil samples used in modeling.

5. Results and Discussion

5.1. Measured Dielectric Properties

Table 3 shows the measured impedance and computed dielectric constant and dielectric loss of soil contaminated by diesel and water content versus frequency. The dielectric properties of the contaminated soil were evaluated in the frequency range from 1 kHz to 1000 kHz. The experimental results indicated that the dielectric properties of soil decrease with increasing the frequency level. The effect of soil water content and diesel contamination level on the measured dielectric constant and dielectric loss at a frequency level of 500 kHz are shown in Figure 7. The experimental results indicated that the dielectric properties of soil increase with as the water and diesel content increase. The response surface of the measured dielectric properties is presented in Figure 8.

Table 3. The measured impedance and computed DC and DL of moist soil contaminated with diesel versus frequency

Frequency (kHz)	Soil impedance (Z)		Dielectric properties	
	R _{soil}	X _{soil}	DC = ε' soil	DL = ε'' soil
1	732.73	-35.16	19762.35	117459.45
100	663.31	-13.09	61.82	1403.12
200	659.30	-20.47	45.63	706.46
300	650.03	-25.49	39.25	480.79
400	643.79	-30.86	35.32	363.04
500	639.26	-37.57	34.34	294.36
600	631.38	-41.64	32.38	245.30
700	624.44	-47.25	31.40	215.86
800	616.24	-53.06	31.40	186.43
900	599.40	-62.10	34.34	166.80
1000	596.33	-44.75	23.55	156.99

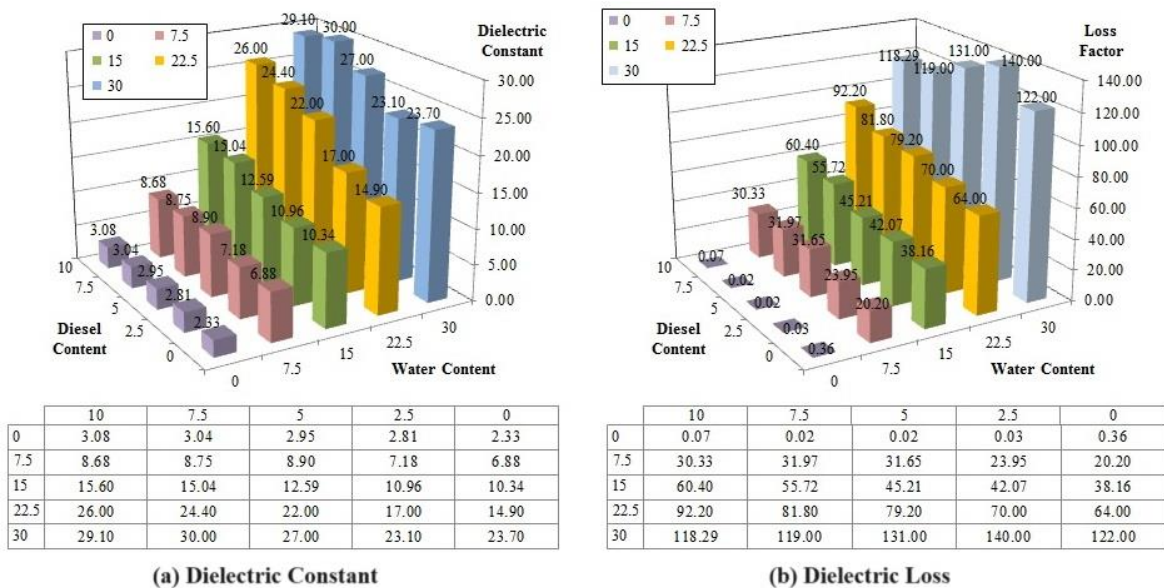


Figure 7. The measured DC and DL of soil contaminated with diesel and various water content at a frequency of 500 kHz

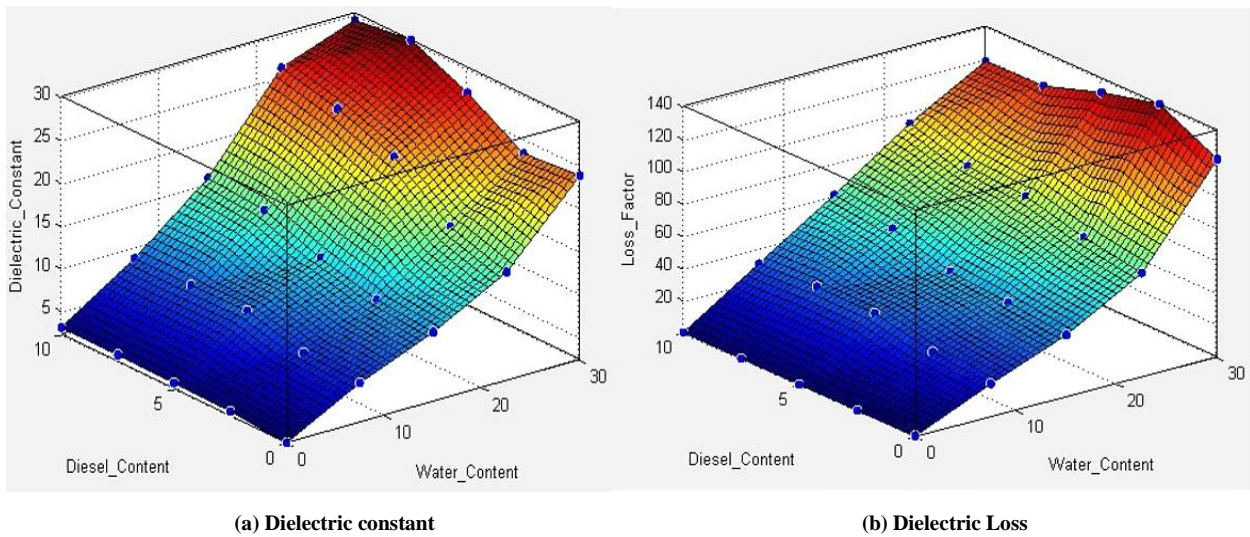


Figure 8. The response surface of DC and DL of soil contaminated with diesel and various water content at a frequency of 500 kHz, (a) Dielectric constant, (b) dielectric loss

5.2. Theoretical Models of Dielectric Properties

Five commonly used theoretical mixture models (Silberstein, Birchak, Looyenga, Lichtenecker, and general power) were investigated to compute the dielectric constant and loss of diesel-contaminated soil based on the dielectric properties of individual components and their volume fractions. The results of the experimental and computing dielectric properties of contaminated soil are shown in Figure 9. The performance fit of the models, including R and MSE, is given in Table 4. The best mixture models were the general power model with power 0.9 for dielectric constant and 1.41 for dielectric loss, followed by the Silberstein Model. All other theoretical mixture models underestimated the dielectric properties of the soil.

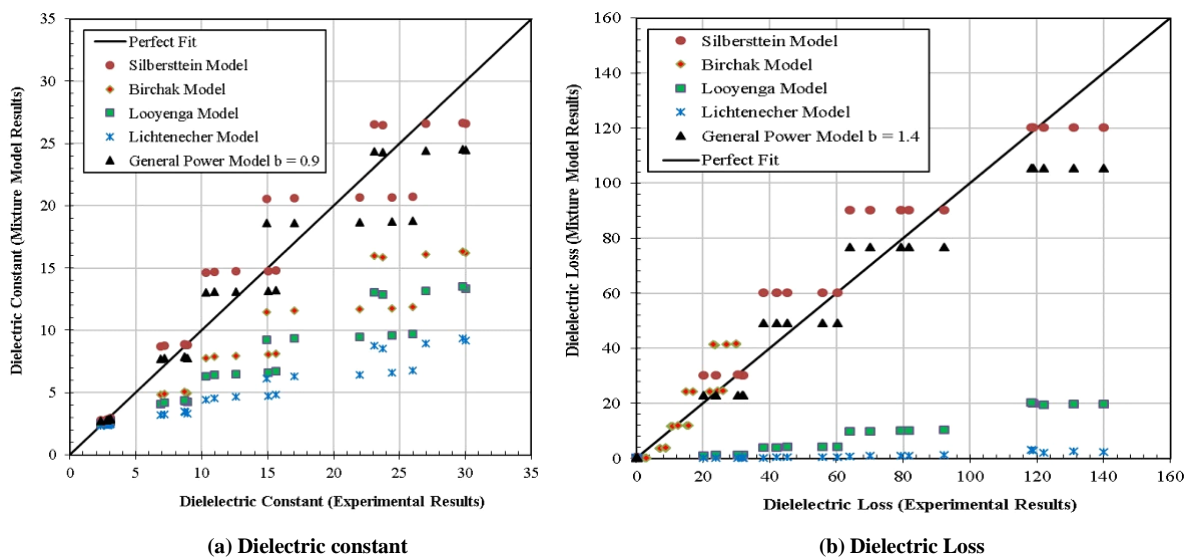


Figure 9. Fitting of the computing dielectric constant and loss factor using theoretical mixture models, (a) Dielectric constant, (b) dielectric loss

Table 4. The performance parameters (MSE and R) for the theoretical mixture models

Theoretical Model (Mixture theory)	Dielectric Constant (DC or ϵ')		Dielectric Loss (DL or ϵ'')	
	MSE	R	MSE	R
Silberstein Model	6.95154	0.9163	121.3031	0.947
Birchak Model	52.1394	0.9249	2426.376	0.8861
Looyenga Model	79.49871	0.9261	3747.878	0.9329
Lichtenecker Model	128.3554	0.9328	4885.997	0.8486
General Power Model $\alpha = 0.9$ and 1.4	8.149957	0.9198	139.9646	0.9553

5.3. Empirical Models of Dielectric Properties

Four empirical quadratic models were investigated using response surface methodology. The degree of fitting of the four empirical models, namely linear, pure quadratic, interaction, and full quadratic model, for both dielectric constant and dielectric loss are shown in Figure 10-a and 10-b, respectively. The performance criteria such as MSE and R are shown in Table 5. The quadratic empirical models show higher accuracy and capability of predicting dielectric properties of the contaminated soil and determining diesel contamination content when compared to the theoretical models. The best empirical model was the full quadratic model with a correlation coefficient of 0.977 and 0.9663 for dielectric constant and dielectric loss, respectively. The response surface of the best full quadratic models is shown in Figure 11.

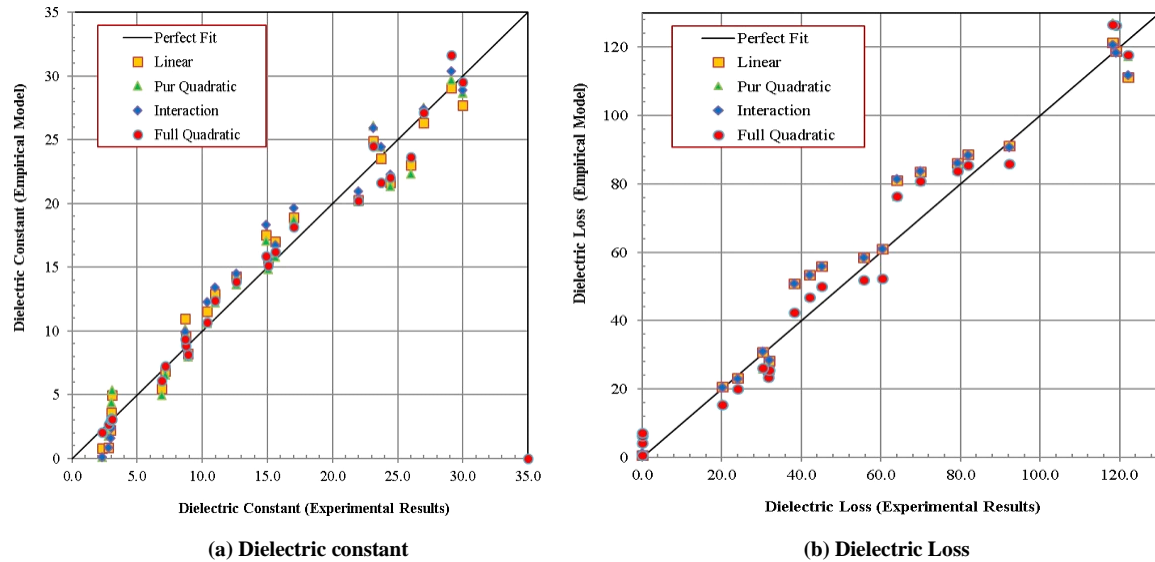


Figure 10. Fitting of the computing dielectric constant and loss factor using empirical models; (a) Dielectric constant, (b) dielectric loss

Table 5. The performance parameters (MSE and R) for the empirical models

Statistical Models (Empirical Models)	Dielectric Constant (DC or ϵ')		Dielectric Loss (DL or ϵ'')	
	MSE	R	MSE	R
Linear Model	2.9728	0.9591	89.32	0.9493
Pure Quadratic Model	2.6972	0.9592	51.44	0.9679
Interaction Model	1.7016	0.9755	89.20	0.9470
Full Quadratic Model	1.4264	0.9773	51.36	0.9663

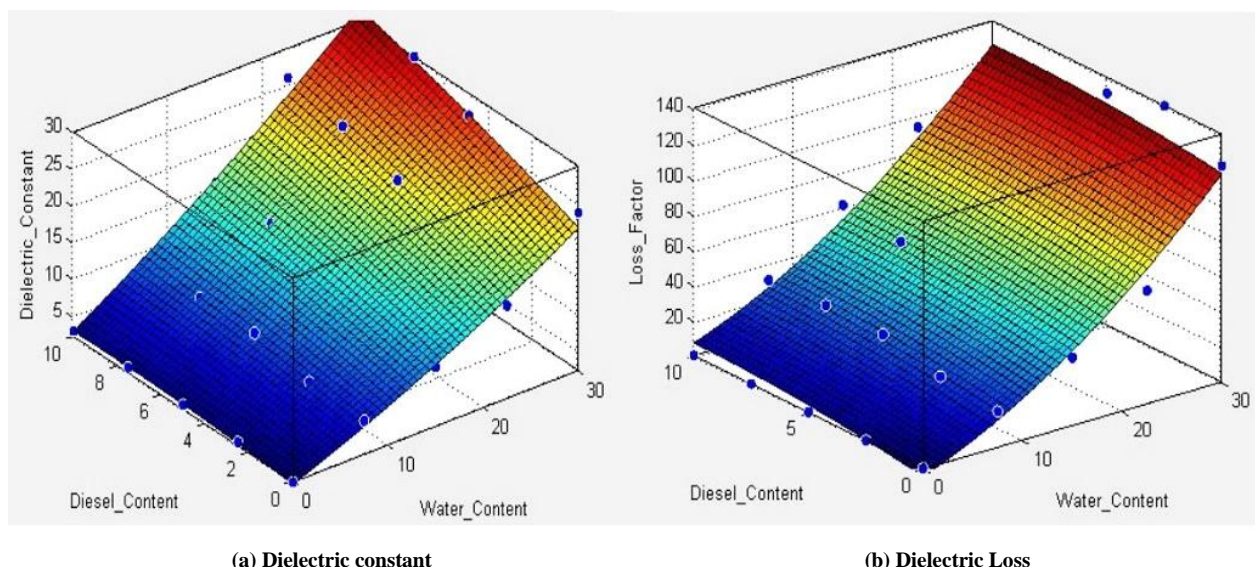


Figure 11. Response surface of the best full quadratic models; (a) Dielectric constant, (b) dielectric loss

5.4. ANN Models

Two ANN modeling methods were investigated using feedforward neural networks (FFNN). The first method was performed to develop an FFNN model to compute the dielectric constant and dielectric loss of diesel-contaminated soil. The model inputs were the volume fraction of the four soil phases, namely solid, air, water, and diesel. Several FFNN models were tried to fit the experimental data. The best FFNN model was the one that contained one hidden layer with 5 neurons, as shown in Figure 12. The performance of the FFNN models was evaluated based on the Mean Square Error (MSE) and coefficient of determination (R) obtained from the training, validation, and testing of overall samples. The MSE is a measure of the average difference between predicted and measured values. It gives an overall idea of the data's spread. The higher the value, the larger the difference between predicted and measured values. R is a measure of how well the predicted values fit the actual data values. The value of R ranges between 0 and 1. If R is closer to 1, then it indicates that there is a strong correlation between the data values and the predicted values. The results of both MSE and R are shown in Figures 13 to 16. The best performance of the network was achieved using FFNN with five neurons and sigmoid and linear correction functions. The correlation of training the ANN was 0.9942. The correlation of the soil sample used for model validation was 0.9967 and 0.9977 for model testing. The overall correlation of FFNN was 0.9933.

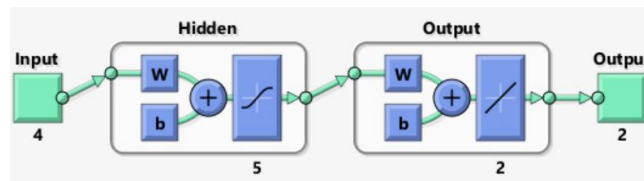


Figure 12. A schematic representation of the used FFNN model for prediction of dielectric properties

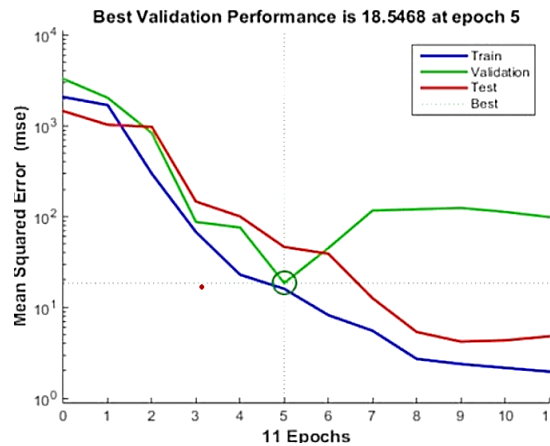


Figure 13. The performance of the used FFNN model for computing DC and DL for soil polluted by diesel and moisture

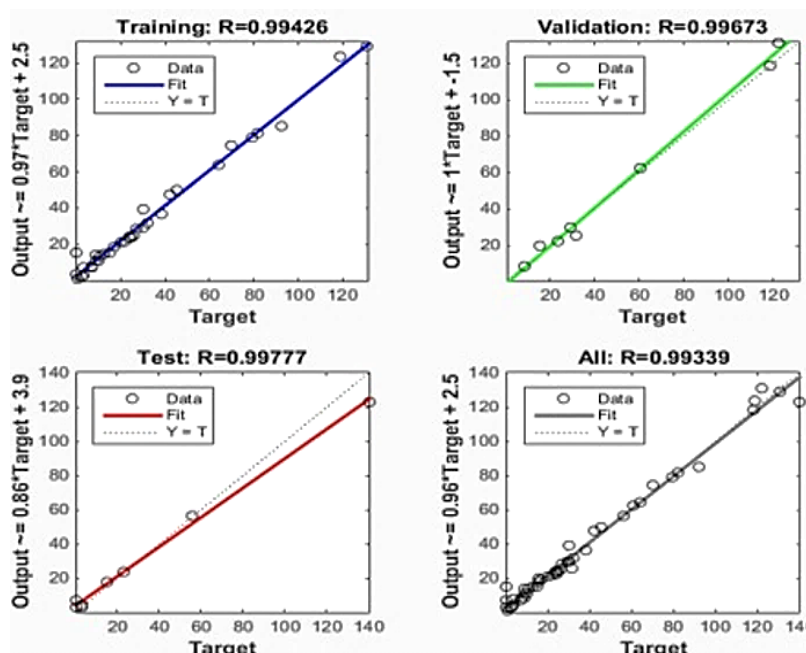


Figure 14. The regression analysis and degree of fit of the used FFNN model for computing DC and DL for soil polluted by diesel and moisture

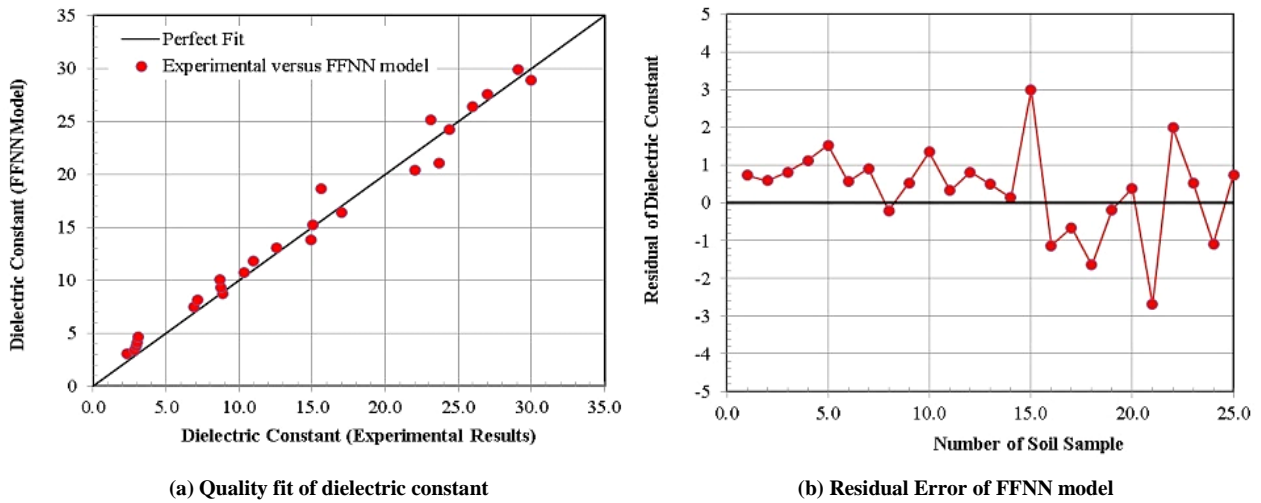


Figure 15. The quality of fitting and residual error of the predicted DC using the FFNN model; (a) Quality fit and (b) Residual Error

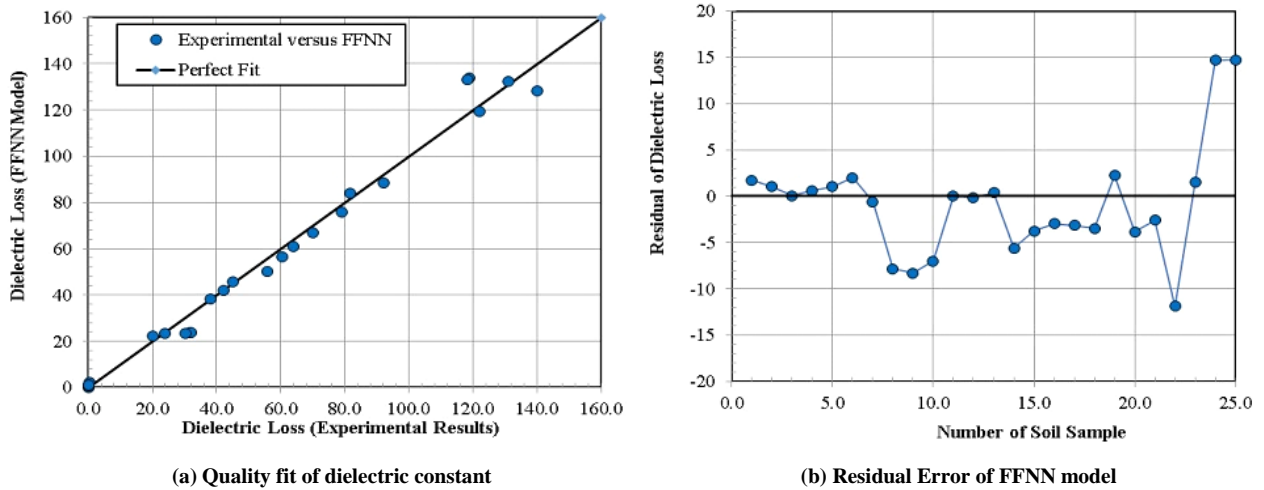


Figure 16. The quality of fit and residual error of the predicted DL using the FFNN model; (a) Quality fit and (b) Residual Error

The second ANN method was used to develop the FFNN models to compute water content and diesel content in the output layer from the measured dielectric constant and dielectric loss as input variables. Figure 17 depicts the FFNN model with 6 neurons in its hidden layer. This model exhibits good predictability of water content and diesel contamination level. The results obtained from this model, as shown in Figures 18 to 21, indicate that the targeted level of performance was achieved at epoch 3, and the error was only 0.003. The best performance of the network was achieved using FFNN with five neurons and sigmoid and linear correction functions. The correlation of training ANN was 0.9657. The correlation of the soil sample used for model validation was 0.9643 and 0.9711 for model testing. The overall correlation of FFNN was 0.9608.

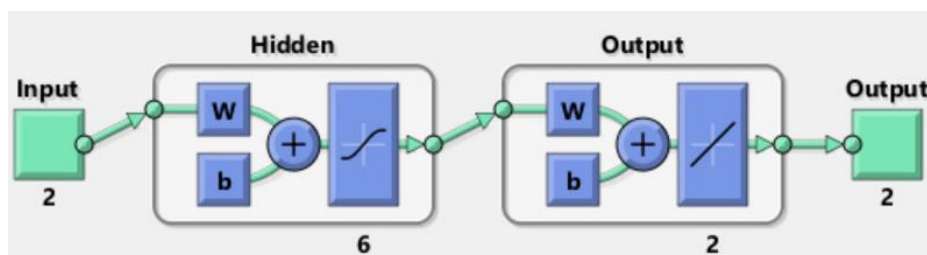


Figure 17. The schematic representation of the used FFNN model for prediction of diesel and water contents

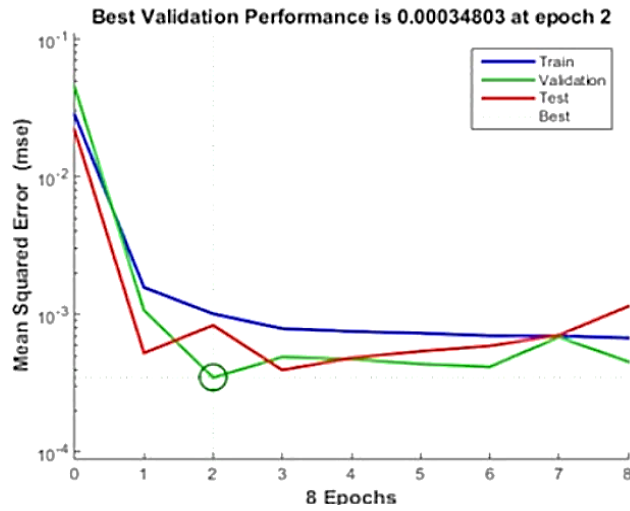


Figure 18. The performance of the used FFNN model for predicting diesel and moisture contents of soil

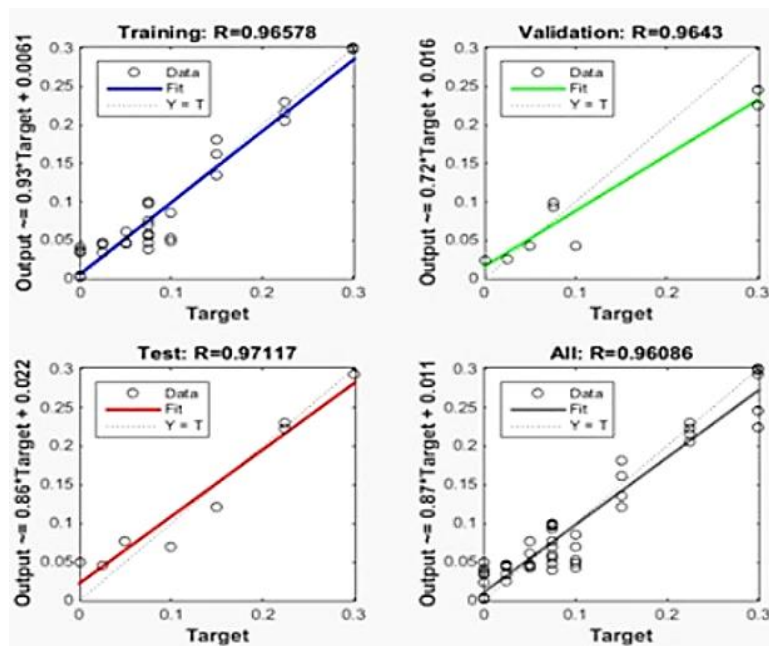


Figure 19. The regression analysis and degree of fit performance of the used FFNN model for predicting diesel and moisture contents of soil

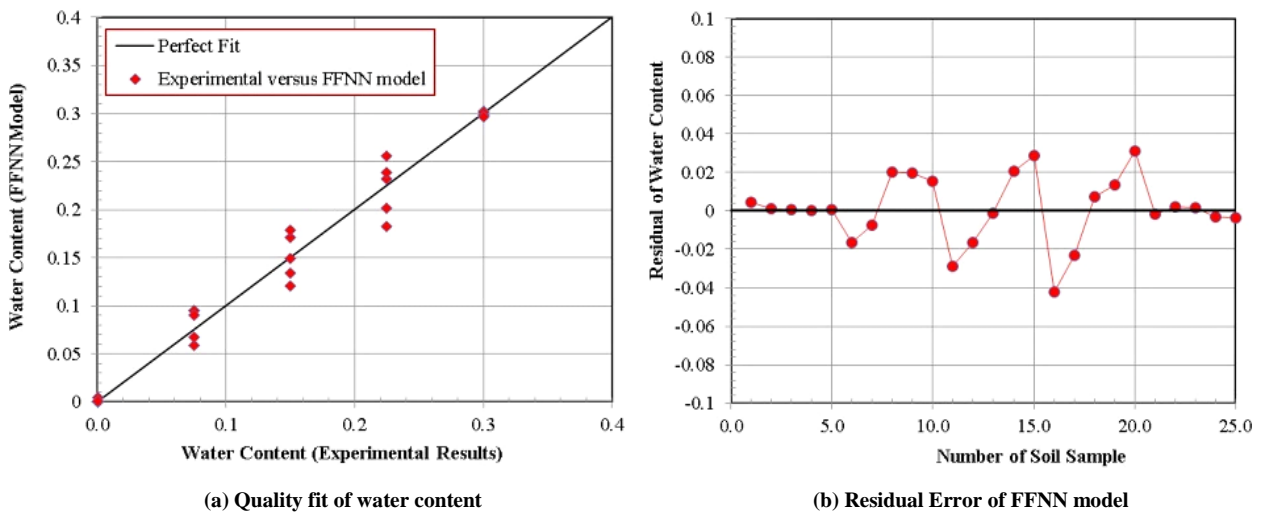


Figure 20. The quality of fit and residual error of the predicted soil water content using the FFNN model; (a) Quality fit and (b) Residual Error

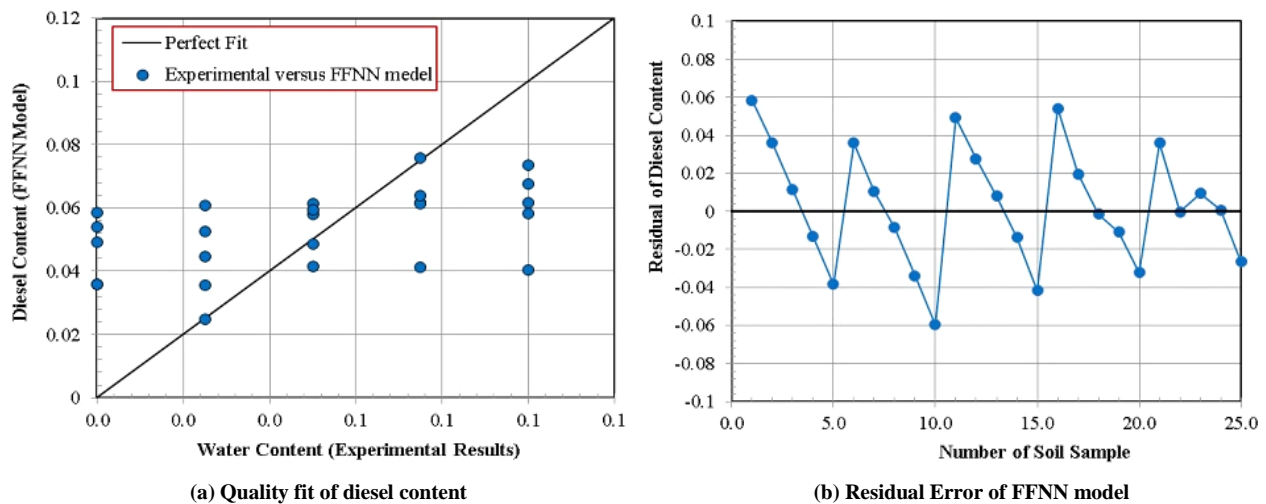


Figure 21. The quality of fit and residual error of the predicted soil diesel content using the FFNN model; (a) Quality fit and (b) Residual Error

6. Conclusion

This study was conducted to compute the dielectric constant and dielectric loss of soil at various water contents and 5 levels of diesel contamination. The dielectric properties of the contaminated soil were evaluated in the frequency range from 1 kHz to 1000 kHz. The experimental results indicate that the dielectric properties of soil decrease with increasing frequency while they increase with increasing water and diesel contents. Three models were used to compute and predict the dielectric properties of the contaminated soil and diesel content. The results of the predicted output using theoretical mixture models, statistical empirical models, and ANN models, lead to the following conclusions:

The best mixture models were the general power model with a power value of 0.9 for the dielectric constant and 1.4 for the dielectric loss, followed by the Silberstein Model. All other theoretical mixture models tended to underestimate the dielectric properties of the soil. The quadratic empirical models, when compared to the theoretical models, show a higher level of accuracy and capability of predicting and computing dielectric properties of contaminated soil and determining diesel contamination content. The best empirical model was the full quadratic model with correlation coefficients of 0.977 and 0.9663 for the dielectric constant and loss, respectively.

The ANN models using feedforward neural networks with 5 and 6 neurons indicate the best computing modeling in determining the dielectric properties of contaminated soil and water content and diesel content, respectively. The correlation of ANN training was 0.9942. The correlation of the soil sample used for model validation was 0.9967 and 0.9977 for model testing. The overall correlation of FFNN was 0.9933.

7. Declarations

7.1. Author Contributions

Conceptualization, H.N., R.I., and H.A.; methodology, H.A., R.I., H.N., and A.R.; software, A.R., M.K., and M.A.; validation H.N. and R.I.; formal analysis, H.N., R.I., A.R., H.A., M.K., R.H., and M.A.; data curation, H.N., M.K., R.H., and H.A.; writing—original draft preparation, H.N., R.I., A.R., H.A., M.K., R.H., and M.A.; writing—review and editing, H.N., R.I., A.R., H.A., M.K., R.H., and M.A.; project administration, H.A. All authors have read and agreed to the published version of the manuscript.

7.2. Data Availability Statement

The data presented in this study are available in the article.

7.3. Funding

The authors received no financial support for the research, authorship, and/or publication of this article.

7.4. Acknowledgements

The authors thank their universities, Yarmouk University, Jordan University, and Jadara University for permitting the use of lab facilities.

7.5. Conflicts of Interest

The authors declare no conflict of interest.

8. References

- [1] Jiang, M., He, L., Niazi, N. K., Wang, H., Gustave, W., Vithanage, M., Geng, K., Shang, H., Zhang, X., & Wang, Z. (2023). Nanobiochar for the remediation of contaminated soil and water: challenges and opportunities. *Biochar*, 5(1), 2. doi:10.1007/s42773-022-00201-x.
- [2] Zhang, X., Gustave, W., He, L., & Yang, X. (2023). Soil pollution, risk assessment and remediation. *Frontiers in Environmental Science*, 11, 1252139. doi:10.3389/978-2-8325-3139-6.
- [3] Schreiber, M. E., & Cozzarelli, I. M. (2021). Arsenic release to the environment from hydrocarbon production, storage, transportation, use and waste management. *Journal of Hazardous Materials*, 411, 125013. doi:10.1016/j.jhazmat.2020.125013.
- [4] Costantini, E. A. C., Castelli, F., Raimondi, S., & Lorenzoni, P. (2002). Assessing Soil Moisture Regimes with Traditional and New Methods. *Soil Science Society of America Journal*, 66(6), 1889–1896. doi:10.2136/sssaj2002.1889.
- [5] Dahim, M., Abuaddous, M., Ismail, R., Al-Mattarneh, H., & Jaradat, A. (2020). Using a Dielectric Capacitance Cell to Determine the Dielectric Properties of Pure Sand Artificially Contaminated with Pb, Cd, Fe, and Zn. *Applied and Environmental Soil Science*, 2020, 1–10. doi:10.1155/2020/8838054.
- [6] Al-Mattarneh, H. M. A., Ghodgaonkar, D. K., & Majid, W. M. B. W. A. (2001). Microwave nondestructive testing for classification of Malaysian timber using free-space techniques. *6th International Symposium on Signal Processing and Its Applications, ISSPA 2001 - Proceedings; 6 Tutorials in Communications, Image Processing and Signal Analysis*, 2, 450–453. doi:10.1109/ISSPA.2001.950177.
- [7] Ismail, R., Al-Mattarneh, H., Malkawi, A. B., Abuaddous, M., Aljamal, M., & Trrad, I. (2024). Prediction Moisture Content and Strength of Wood Using Free-Space Microwave Transmission Line NDT. *2024 21st International Multi-Conference on Systems, Signals & Devices (SSD)*, 47, 492–499. doi:10.1109/ssd61670.2024.10548770..
- [8] Luciani, G., Berardinelli, A., Crescentini, M., Romani, A., Tartagni, M., & Ragni, L. (2017). Non-invasive soil moisture sensing based on open-ended waveguide and multivariate analysis. *Sensors and Actuators, A: Physical*, 265, 236–245. doi:10.1016/j.sna.2017.08.034.
- [9] Al-Mattarneh, H. M. A., Ghodgaonkar, D. K., Abdul Hamid, H., Al-Fugara, A., & Abu Bakar, S. H. (2002). Microwave reflectometer system for continuous monitoring of water quality. *Student Conference on Research and Development*, 40, 430–433. doi:10.1109/scored.2002.1033150.
- [10] Ermeey, A. K., Ghodgaonkar, D. K., & Al-Mattarneh, H. M. A. (2003). Three probe reflectometer algorithm for complex coefficient measurements of water quality at microwave frequencies. *2003 Asia-Pacific Conference on Applied Electromagnetics, APACE 2003 - Proceedings*, 1234481, 113–115. doi:10.1109/APACE.2003.1234481.
- [11] He, H., Aogu, K., Li, M., Xu, J., Sheng, W., Jones, S. B., González-Teruel, J. D., Robinson, D. A., Horton, R., Bristow, K., Dyck, M., ..., Feng, H., Si, B., & Lv, J. (2021). A review of time domain reflectometry (TDR) applications in porous media. *Advances in Agronomy*, Elsevier, Amsterdam, Netherland. doi:10.1016/bs.agron.2021.02.003.
- [12] Kulyandin, G. A., Fedorov, M. P., Savvin, D. V., & Fedorova, L. L. (2021). Identification of Technogenic Pollution of soil Environment by The GPR Method. *Engineering and Mining Geophysics 2021*, 1–5. doi:10.3997/2214-4609.202152089.
- [13] Al-Mattarneh, H., & Alwadie, A. (2016). Development of Low Frequency Dielectric Cell for Water Quality Application. *Procedia Engineering*, 148, 687–693. doi:10.1016/j.proeng.2016.06.554.
- [14] Arora, H. C., Bhushan, B., Kumar, A., Kumar, P., Hadzima-Nyarko, M., Radu, D., ... & Kapoor, N. R. (2024). Ensemble learning based compressive strength prediction of concrete structures through real-time non-destructive testing. *Scientific reports*, 14(1), 1824. doi:10.1038/s41598-024-52046-y.
- [15] Al-Mattarneh, H. M. A., Ghodgaonkar, D. K., & Majid, W. M. B. W. A. (2001). Determination of compressive strength of concrete using free-space reflection measurements in the frequency range of 8 - 12.5 GHz. *Asia-Pacific Microwave Conference Proceedings, APMC*, 2, 679–682. doi:10.1109/apmc.2001.985463.
- [16] Al-Mattarneh, H., Ismail, R., Nuruddin, M., Shafiq, N., & Dahim, M. (2016). Characterization of Pb and Cd contaminated sandy soil by dielectric means. *Engineering Challenges for Sustainable Future*, CRC Press, Boca Raton, United States doi:10.1201/b21942-65.
- [17] Ismail, R., Dahim, M., Jaradat, A., Hatamleh, R., Telfah, D., Abuaddous, M., & Al-Mattarneh, H. (2021). Field Dielectric Sensor for Soil Pollution Application. *IOP Conference Series: Earth and Environmental Science*, 801(1), 012003. doi:10.1088/1755-1315/801/1/012003.
- [18] Dahim, M., Abuaddous, M., Al-Mattarneh, H., Rawashdeh, A., & Ismail, R. (2021). Enhancement of road pavement material using conventional and nano-crude oil fly ash. *Applied Nanoscience (Switzerland)*, 11(10), 2517–2524. doi:10.1007/s13204-021-02103-z.

- [19] Telfah, D., Al-Mattarneh, H., Ismail, R., Rawashdeh, A., Aljamal, M., & Dahim, M. (2024). Development of permittivity sensor for advanced in situ testing and evaluation of building material. 2024 21st International Multi-Conference on Systems, Signals & Devices (SSD), 120, 164–169. doi:10.1109/ssd61670.2024.10548329.
- [20] Malkawi, A. B., Nuruddin, M. F., Fauzi, A., Al-Mattarneh, H., & Mohammed, B. S. (2017). Effect of plasticizers and water on properties of HCFA geopolymers. *Key Engineering Materials*, 733 KEM, 76–79. doi:10.4028/www.scientific.net/KEM.733.76.
- [21] Abdullahi, M., Al-Mattarneh, H. M. A., & Mohammed, B. S. (2009). Equations for mix design of structural lightweight concrete. *European Journal of Scientific Research*, 31(1), 132–141.
- [22] Zain, M. F. M., Karim, M. R., Islam, M. N., Hossain, M. M., Jamil, M., & Al-Mattarneh, H. M. A. (2015). Prediction of strength and slump of silica fume incorporated high-performance concrete. *Asian Journal of Scientific Research*, 8(3), 264–277. doi:10.3923/ajsr.2015.264.277.
- [23] Monjardin, C. E. F., Power, C., Senoro, D. B., & De Jesus, K. L. M. (2023). Application of Machine Learning for Prediction and Monitoring of Manganese Concentration in Soil and Surface Water. *Water (Switzerland)*, 15(13), 2318. doi:10.3390/w15132318.
- [24] Pham, B. T., Singh, S. K., & Ly, H. B. (2020). Using artificial neural network (ANN) for prediction of soil coefficient of consolidation. *Vietnam Journal of Earth Sciences*, 42(4), 311–319. doi:10.15625/0866-7187/42/4/15008.
- [25] Ayoubi, S., Pilehvar, A., Mokhtari, P., & L., K. (2011). Application of Artificial Neural Network (ANN) to Predict Soil Organic Matter Using Remote Sensing Data in Two Ecosystems. *Biomass and Remote Sensing of Biomass*, Intech open, London, United Kingdom. doi:10.5772/18956.
- [26] Carvalho, M. G., Barreto, E. M. do R., Ferreira, J. A. da C., França, F. A. N. de, & Freitas Neto, O. de. (2022). Applications of artificial intelligence in the determination of soil shear strength parameters: a systematic mapping of the literature. *Research, Society and Development*, 11(1), e27711124506. doi:10.33448/rsd-v11i1.24506.
- [27] Negiş, H. (2024). Using Models and Artificial Neural Networks to Predict Soil Compaction Based on Textural Properties of Soils under Agriculture. *Agriculture (Switzerland)*, 14(1), 47. doi:10.3390/agriculture14010047.
- [28] Li, B., You, Z., Ni, K., & Wang, Y. (2024). Prediction of Soil Compaction Parameters Using Machine Learning Models. *Applied Sciences (Switzerland)*, 14(7), 2716. doi:10.3390/app14072716.
- [29] Wrzesiński, G., & Markiewicz, A. (2022). Article Prediction of Permeability Coefficient k in Sandy Soils Using ANN. *Sustainability (Switzerland)*, 14(11), 6736. doi:10.3390/su14116736.
- [30] Bieganski, A., Józefaciuk, G., Bandura, L., Guz, Ł., Łagód, G., & Franus, W. (2018). Evaluation of hydrocarbon soil pollution using e-nose. *Sensors (Switzerland)*, 18(8), 2463. doi:10.3390/s18082463.
- [31] Han, H., Choi, C., Kim, J., Morrison, R. R., Jung, J., & Kim, H. S. (2021). Multiple-depth soil moisture estimates using artificial neural network and long short-term memory models. *Water (Switzerland)*, 13(18), 2584. doi:10.3390/w13182584.
- [32] Wang, Z., Zhang, W., & He, Y. (2023). Soil Heavy-Metal Pollution Prediction Methods Based on Two Improved Neural Network Models. *Applied Sciences (Switzerland)*, 13(21), 11647. doi:10.3390/app132111647.
- [33] Hippel, A. V. (1954). *Dielectric materials and applications*. Artech House, London, United Kingdom.
- [34] Pandey, G., Weber, R. J., & Kumar, R. (2018). Agricultural Cyber-Physical System: In-Situ Soil Moisture and Salinity Estimation by Dielectric Mixing. *IEEE Access*, 6, 43179–43191. doi:10.1109/access.2018.2862634.
- [35] Mironov, V. L., Kosolapova, L. G., & Fomin, S. V. (2009). Physically and mineralogically based spectroscopic dielectric model for moist soils. *IEEE Transactions on Geoscience and Remote Sensing*, 47(7), 2059–2070. doi:10.1109/TGRS.2008.2011631.
- [36] Zhang, L., Meng, Q., Hu, D., Zhang, Y., Yao, S., & Chen, X. (2020). Comparison of different soil dielectric models for microwave soil moisture retrievals. *International Journal of Remote Sensing*, 41(8), 3054–3069. doi:10.1080/01431161.2019.1698077.
- [37] Cole, K. S., & Cole, R. H. (1941). Dispersion and absorption in dielectrics I. Alternating current characteristics. *The Journal of Chemical Physics*, 9(4), 341–351. doi:10.1063/1.1750906.
- [38] Hong, T., Tang, Z., Zhou, Y., Zhu, H., & Huang, K. (2019). Dielectric relaxation of interacting/polarizable polar molecules with linear reaction dynamics in a weak alternating field. *Chemical Physics Letters*, 727, 66–71. doi:10.1016/j.cplett.2019.04.053.
- [39] Umoh, G. V., Leal-Perez, J. E., Olive-Méndez, S. F., González-Hernández, J., Mercader-Trejo, F., Herrera-Basurto, R., Auciello, O., & Hurtado-Macias, A. (2022). Complex dielectric function, Cole-Cole, and optical properties evaluation in BiMnO₃ thin-films by Valence Electron Energy Loss Spectrometry (VEELS) analysis. *Ceramics International*, 48(15), 22182–22187. doi:10.1016/j.ceramint.2022.04.212.
- [40] Chenaf, D., & Amara N. (2001). Time domain Reflectometry for the Characterisation of Diesel Contaminated Soils. *Proceedings TDR 2001, Second International Symposium and Workshop on Time Domain Reflectometry for innovative Geotechnical Applications*, 5-7 September, 2001, Northwestern University in Evanston, Illinois, United States.

- [41] Sihvola, A. (1999). *Electromagnetic Mixing Formulas and Applications*. Electromagnetic Mixing Formulas and Applications. The Institution of Engineering and Technology, London, United Kingdom. doi:10.1049/pbew047e.
- [42] Birchak, J. R., Gardner, C. G., Hipp, J. E., & Victor, J. M. (1974). High Dielectric Constant Microwave Probes for Sensing Soil Moisture. *Proceedings of the IEEE*, 62(1), 93–98. doi:10.1109/PROC.1974.9388.
- [43] Looyenga, H. (1965). Dielectric constants of heterogeneous mixtures. *Physica*, 31(3), 401–406. doi:10.1016/0031-8914(65)90045-5.
- [44] Zakri, T., Laurent, J. P., & Vauclin, M. (1998). Theoretical evidence for “Lichtenecker’s mixture formulae” based on the effective medium theory. *Journal of Physics D: Applied Physics*, 31(13), 1589–1594. doi:10.1088/0022-3727/31/13/013.
- [45] Topp, G. C. (2003). State of the art of measuring soil water content. *Hydrological Processes*, 17(14), 2993–2996. doi:10.1002/hyp.5148.
- [46] Woodhead, I. M., Buchan, G. D., Christie, J. H., & Irie, K. (2003). A General Dielectric Model for Time Domain Reflectometry. *Biosystems Engineering*, 86(2), 207–216. doi:10.1016/S1537-5110(03)00131-4.
- [47] Tenza-Abril, A. J., Benavente, D., Pla, C., Baeza-Brotos, F., Valdes-Abellan, J., & Solak, A. M. (2020). Statistical and experimental study for determining the influence of the segregation phenomenon on physical and mechanical properties of lightweight concrete. *Construction and Building Materials*, 238, 117642. doi:10.1016/j.conbuildmat.2019.117642.
- [48] Nuruddin, M., Malkawi, A., Fauzi, A., Mohammed, B., & Al-Mattarneh, H. (2016). *Effects of alkaline solution on the microstructure of HCFA geopolymers*. *Engineering Challenges for Sustainable Future*, CRC Press, Boca Raton, United States. doi:10.1201/b21942-102.
- [49] Yasin, A. A., Awwad, M. T., Malkawi, A. B., Maraqa, F. R., & Alomari, J. A. (2023). Optimization of Tuff Stones Content in Lightweight Concrete Using Artificial Neural Networks. *Civil Engineering Journal (Iran)*, 9(11), 2823–2833. doi:10.28991/CEJ-2023-09-11-013.
- [50] Najjar, Y. M., & Ali, H. E. (1998). CPT-based liquefaction potential assessment: A neuronet approach. *Geotechnical Earthquake Engineering and Soil Dynamics III*, 1, 542–553.
- [51] Sivakugan, N., Eckersley, J., & Li, H. (1998). Settlement predictions using neural networks. *Australian Civil Engineering Transactions*, 40, 49-52.
- [52] Sinha, S. K., & Wang, M. C. (2008). Artificial neural network prediction models for soil compaction and permeability. *Geotechnical and Geological Engineering*, 26(1), 47–64. doi:10.1007/s10706-007-9146-3.
- [53] Ismail, R. (2024). Improving wastewater treatment plant performance: an ANN-based predictive model for managing average daily overflow and resource allocation optimization using Tabu search. *Asian Journal of Civil Engineering*, 25(2), 1427–1441. doi:10.1007/s42107-023-00853-5.